



ELSEVIER

Available online at [www.sciencedirect.com](http://www.sciencedirect.com)

SCIENCE @ DIRECT®

Journal of Magnetism and Magnetic Materials 280 (2004) 404–411

Journal of  
magnetism  
and  
magnetic  
materials

[www.elsevier.com/locate/jmmm](http://www.elsevier.com/locate/jmmm)

# Structure, magnetic and transport properties of $\text{La}_{1-x}\text{Bi}_x\text{MnO}_3$

Y.D. Zhao<sup>\*</sup>, Jonghyuk Park, R.-J. Jung, H.-J. Noh, S.-J. Oh

*Department of Physics and Center for Strongly Correlated Materials Research, Seoul National University, Seoul 151-742, South Korea*

Received 20 May 2003; received in revised form 29 February 2004

## Abstract

We have investigated the structural, magnetic and transport properties of  $\text{La}_{1-x}\text{Bi}_x\text{MnO}_3$  samples. As the Bi content increases, a structural transition from rhombohedral to pseudocubic and a magnetic phase transition from ferromagnetic ordering to cluster glass are identified. Metal–insulator (MI) transitions and large magnetoresistance (MR) effects are observed at low Bi doping levels, while insulating behavior of resistivity is found in the whole measured temperature range at high-doping levels. Two distinct ferromagnetic insulating (FI) states are found at low temperatures in this system. One can be suppressed and the other can be enhanced by applying magnetic fields. Possible reasons for the observed structural, magnetic phase transitions and changes of resistivity behavior with Bi doping are discussed.

© 2004 Elsevier B.V. All rights reserved.

PACS: 75.47.Gk; 75.47.Lx; 72.80.Ga; 71.30.+h

Keywords: Colossal magnetoresistance; Manganites; Metal–insulator transitions

## 1. Introduction

In recent years, there has been a lot of interest in rare-earth manganese perovskites due to their potential technological applications and the fascinating physical phenomena they exhibit such as colossal magnetoresistance (CMR), metal–insulator (MI)

transition, charge ordering (CO) and orbital ordering (OO) [1–5]. The interplay between magnetic, transport and structural properties gives rise to the above-mentioned complex phenomena. One of the most extensively studied systems is the  $\text{La}_{1-x}\text{A}_x\text{MnO}_3$  series of compounds, where A constitutes trivalent or divalent cations. The undoped  $\text{LaMnO}_3$  is an antiferromagnetic insulator. The correct structure for stoichiometric  $\text{LaMnO}_3$  at room temperature is orthorhombic. When doped with divalent cations on the La sites,

<sup>\*</sup>Corresponding author. Tel.: +82-288-08985; fax: +82-287-76796.

E-mail address: [zhaoyd@escalab.snu.ac.kr](mailto:zhaoyd@escalab.snu.ac.kr) (Y.D. Zhao).

Table 1  
Lattice constants and other selected parameters of structure for  $\text{La}_{1-x}\text{Bi}_x\text{MnO}_3$  compounds

$X$	$a$ (nm)	$\alpha$ ( $^\circ$ )	$V$ ( $10^{-3} \text{ nm}^3$ )	$\langle r_A \rangle$ (nm)	$t$	$\sigma^2$ ( $10^{-7} \text{ nm}^2$ )
0.10	0.5503(2)	59.76(1)	117.18(1)	0.1222	0.9133	3.6
0.20	0.5508(2)	59.79(2)	117.60(1)	0.1224	0.9140	6.4
0.25	0.5512(1)	59.83(1)	117.96(1)	0.1225	0.9144	7.5
0.40	0.5520(1)	59.97(1)	118.84(2)	0.1228	0.9154	9.6
0.50	0.55232(7)	60.02(1)	119.21(1)	0.1230	0.9161	10.0
0.60	0.55320(5)	60.12(1)	120.03(2)	0.1232	0.9168	9.6

Note that  $\langle r_A \rangle$ ,  $t$  and  $\sigma^2$  are calculated from cationic radii  $r(\text{La}^{3+}) = 0.122 \text{ nm}$  and  $r(\text{Bi}^{3+}) = 0.124 \text{ nm}$ .

a remarkable transition from a paramagnetic insulator (PI) phase to a ferromagnetic metal (FM) phase occurs below the Curie temperature  $T_c$ . This transition has been explained by the double exchange (DE) interaction between  $\text{Mn}^{3+}$  and  $\text{Mn}^{4+}$  ions [6]. The hole concentration, the average size of A-site cations  $\langle r_A \rangle$  and the size mismatch at the A-site represented by the variance  $\sigma^2 = \langle r_A^2 \rangle - \langle r_A \rangle^2$  are found to be three important factors that govern the physical properties of these manganites [7–9]. On the other hand, another perovskite-type manganese compound  $\text{BiMnO}_3$  exhibits a very different structure and properties. It is a ferromagnetic insulator with a Curie temperature of 105–110 K. The observed magnetic moment at 5 K and 5 T reaches  $3.6 \mu_B$ , slightly smaller than the fully aligned spin moment  $4 \mu_B$  for  $\text{Mn}^{3+}$  [10,11]. It has a triclinic structure at room temperature and the origin of its ferromagnetism is still not clear. Recent work [12] showed that the  $\text{MnO}_6$  octahedra in  $\text{BiMnO}_3$  are fairly distorted from the regular ones. The authors suggested that the strongly polarized Bi lone pair electrons are responsible for the heavily distorted triclinic structure of  $\text{BiMnO}_3$ . When doped with divalent cations (such as Ca, Sr) on the Bi sites, no MI transition is observed. Instead, strong charge ordering is easily found over a broad doping range [13,14]. It was also found that the average  $\text{MnO}_6$  octahedra in these doped Bi-containing manganites are about 0.5% larger than those of the La analogous. The replacement of La by Bi causes an increase of the average Mn–O–Mn distortion. The lone pair electrons were suggested to play a role in these compounds [13].

It is interesting to investigate the intermediate compounds  $\text{La}_{1-x}\text{Bi}_x\text{MnO}_3$  (LBMO) between the two end compounds. This system was first briefly studied by Troyanchuk et al. [15] and only ferromagnetism was addressed. However, we think this system is worthy of detailed investigation because the two end compounds have very different structures and properties although  $\text{Bi}^{3+}$  is expected to substitute  $\text{La}^{3+}$  completely due to their isovalence and very similar ionic radii found in many oxides [16]. In particular, Bi doping does not introduce holes into the system and causes only very small A-site cationic mismatch (Table 1). In this work, we investigate in detail the structure, resistivity and magnetic property of LBMO. We observed large magnetoresistance effects in this system. We also found two distinct ferromagnetic insulating (FI) states at low temperatures.

## 2. Experimental

Polycrystalline samples of nominal composition  $\text{La}_{1-x}\text{Bi}_x\text{MnO}_3$  were synthesized by conventional solid-state reaction in air. Highly pure powders of  $\text{La}_2\text{O}_3$ ,  $\text{Bi}_2\text{O}_3$  and  $\text{MnO}_2$  were mixed and ground, then fired at 900–1000  $^\circ\text{C}$  for 30 h with several intermediate grindings. The sintered mixtures were reground, pelletized and sintered at 1100–1200  $^\circ\text{C}$  for 12 h followed by furnace-cooling to room temperature at a rate of 5  $^\circ\text{C}/\text{min}$ . X-ray powder diffraction (XRD) experiments were carried out on Rigaku D/Max-3C using Cu K radiation, 40 kV accelerating voltage and 30 mA working current. Magnetic property was measured with a Quantum

Design MPMS SQUID magnetometer. Magnetization measurements were performed in both a zero-field-cooled (ZFC) and a field-cooled (FC) mode in a field of 100 G. The resistivity of samples under fields up to 5 T was measured between 5 and 300 K by the standard four-probe method. The magnetic field direction was parallel to the current direction.

### 3. Experimental results

The X-ray diffraction analyses of our samples show that single-phase samples can be obtained for  $x < 0.6$ . When  $x \geq 0.6$ , impurity phase ( $\text{Bi}_2\text{O}_3$ ) starts to appear with an amount of about 6% (estimated from the integral intensity of peaks). In Fig. 1 we show some XRD patterns of these samples. This indicates that Bi behaves very differently and cannot substitute La completely at ambient conditions although they are very similar in valence and ionic radius, consistent with the fact that  $\text{BiMnO}_3$  can only be synthesized under high pressure [10–12]. We found all our samples can be well indexed using a rhombohedral

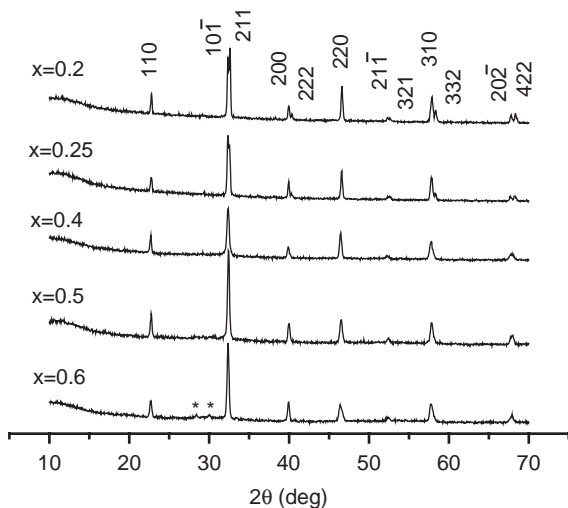


Fig. 1. Room temperature X-ray powder diffraction patterns for  $x = 0.2, 0.25, 0.4, 0.5$  and  $0.6$ . Rhombohedral symmetry is identified for these samples. The marked peaks come from impurity phase  $\text{Bi}_2\text{O}_3$ .

cell. As the Bi content increases the lattice constant  $a$ , cell volume  $V$  and the rhombohedral angle  $\alpha$  also increase linearly (see Table 1). Actually, when  $x = 0.5$ , the angle is very close to  $60^\circ$  and the peaks can also be well indexed using a cubic cell, but the observed intensities of the Bragg reflections cannot be explained within the cubic symmetry. We may call the symmetry of this sample pseudocubic. As the Bi content continues to increase, the angle becomes larger than  $60^\circ$ . Taking into account that  $\text{BiMnO}_3$  is triclinic, we can expect the symmetry to be further divergent from cubic as  $x$  increases from 0.6 to 1.0. Apparently, the symmetry evolution should not be attributed to the slight increase of tolerance factor  $t$  with increasing Bi content (see Table 1). Pseudocubic phases were also observed in  $\text{La}_{0.88}\text{Sr}_{0.12}\text{MnO}_3$  [17] at both low and high temperatures. In these phases the cooperative Jahn–Teller (JT) distortion is very small or even removed. As stated earlier, Bi-doping causes the enhancement of Mn–O–Mn distortion, therefore reducing the range of the cooperative JT distortion. This seems the reason why we see the pseudocubic symmetry at  $x = 0.5$ .

An early study of  $\text{LaMnO}_3$  [18] showed that when the percentage of  $\text{Mn}^{4+}$  is larger than 20%, the room temperature structure is rhombohedral. Recent work on  $\text{LaMnO}_{3+\delta}$  [19] showed that stoichiometric  $\text{LaMnO}_3$  should be prepared in the absence of oxygen. Sintering in air inevitably results in nonstoichiometric  $\text{LaMnO}_{3+\delta}$  with  $\delta > 0$ .  $\delta$  depending on the sintering temperature. Lower sintering temperature will lead to higher  $\delta$ . When  $\delta \geq 0.09$ , the rhombohedral structure is observed with both the rhombohedral angle  $\alpha$  and the lattice constant  $a$  decreasing with rising  $\delta$ . Actually, the real composition of  $\text{LaMnO}_{3+\delta}$  should be better expressed in terms of cationic vacancies other than excess oxygen, i.e.,  $\text{La}_{1-\eta}\text{Mn}_{1-\eta}\text{O}_3$  with  $\eta = \delta/(3 + \delta)$  [20]. Taking the volatility of Bi into account, it is reasonable that there are  $\text{Mn}^{4+}$  ions and cationic vacancies in our samples, which are related to the rhombohedral structure of these samples. It should be pointed out that the cell volume in Ref. [19] decreases with the increase of cationic vacancy  $\eta$  (or  $\delta$ ) (see Table 1 of Ref. [19]). In contrast, the expansion of cell volume with increasing Bi

content was found in our samples (Table 1). Compared with undoped  $\text{LaMnO}_{3+\delta}$ , the lattice constant of our samples is larger. These results suggest that the doping of Bi is an important factor which leads to the expansion of cell volume. It was established [16] that the effective ionic radius of  $\text{Bi}^{3+}$  depends on the character of the  $6s^2$  lone pair. When the lone pair character is dominant  $r(\text{Bi}^{3+}) = 0.124 \text{ nm}$  (CN=9), which is bigger than  $r(\text{La}^{3+}) = 0.122 \text{ nm}$  (CN=9); when the lone pair character is constrained,  $r(\text{Bi}^{3+}) = 0.116 \text{ nm}$  (CN=9). So it is reasonable to conclude that the  $6s^2$  lone pair character is dominant in our samples.

Fig. 2 shows the temperature dependence of magnetization  $M$  for  $x = 0.2, 0.25, 0.4, 0.5$ . All samples exhibit a paramagnetic to ferromagnetic

transition when temperature is lower than a critical temperature  $T_c$ , which is 167, 156, 96 and 80 K for  $x = 0.2, 0.25, 0.4$  and  $0.5$ , respectively (here  $T_c$  is defined as the mid-temperature of the transition range). Ferromagnetism is apparently due to the DE interaction between  $\text{Mn}^{3+}$  and  $\text{Mn}^{4+}$  ions in these samples, as suggested in the previous work [15]. As the Bi content increases, both  $T_c$  and the magnetization  $M$  decrease. Meanwhile, the divergence between the FC and the ZFC measurements at 20 K is also enhanced, indicating the departure from a good ferromagnet. Ferromagnetism was also observed in nonstoichiometric  $\text{LaMnO}_{3+\delta}$  [19], however, there is no simple relation between  $\delta$  and  $T_c$  or saturation magnetization. Both spin glass (SG) behavior and metamagnetic canted spin (MCS) behavior were found in lower and high  $\delta$  regions, respectively. Spin glass behavior was also observed in highly defective  $\text{La}_{1-x}\text{Mn}_{1-y}\text{O}_3$  [21]. In LBMO, the magnetization behavior of the  $x = 0.4$  and  $0.5$  samples is different from the SG behavior because we didn't observe the cusp in their ZFC curves, which is a characteristic feature of SG behavior [22]. Besides, in canonical SG systems the FC magnetization shows a nearly constant value below the irreversibility temperature  $T_r$  at which ZFC and FC curves merge, but the FC magnetization of these samples increase strongly below  $T_r$ . A similar phenomenon was found in  $\text{La}_{0.7-x}\text{Y}_x\text{Ca}_{0.3}\text{MnO}_3$  [23], where as  $x$  increased there was a gradual trend toward reduced magnetization and when  $x = 0.15$  the magnetic behavior was very similar to that of our  $x = 0.5$  sample. This magnetization behavior was interpreted as a cluster glass behavior because both magnetization relaxation and aging effects found in these compounds give evidence of the existence of magnetic clusters.

Fig. 3 shows the temperature dependence of resistivity with and without external magnetic fields for the  $x = 0.2, 0.25, 0.4$  and  $0.5$  samples. When  $H = 0$ , the resistivity increases rapidly as the Bi content increases. Insulating behavior of resistivity is found for  $x \geq 0.4$  in the whole measured temperature range (in Fig. 3(c) only the data at  $T > 120 \text{ K}$  are showed). When  $x = 0.2$ , the sample undergoes transitions from an insulating state to a metal-like state below  $T_1 = 155 \text{ K}$  and then to another insulating state below

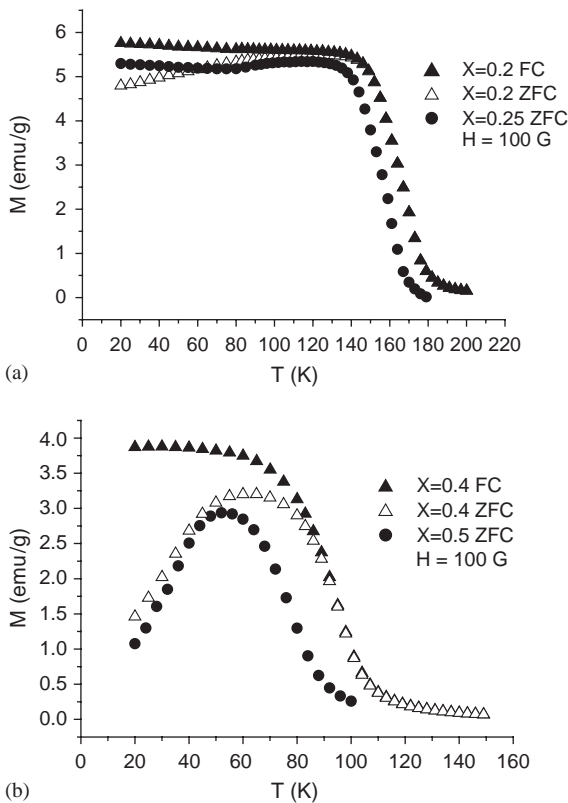


Fig. 2. Temperature dependence of d.c. magnetization  $M(T)$  for  $x = 0.2, 0.25, 0.4$  and  $0.5$ . The data were collected in a field-cooled (FC) and zero-field-cooled (ZFC) mode under a magnetic field of 100 G.

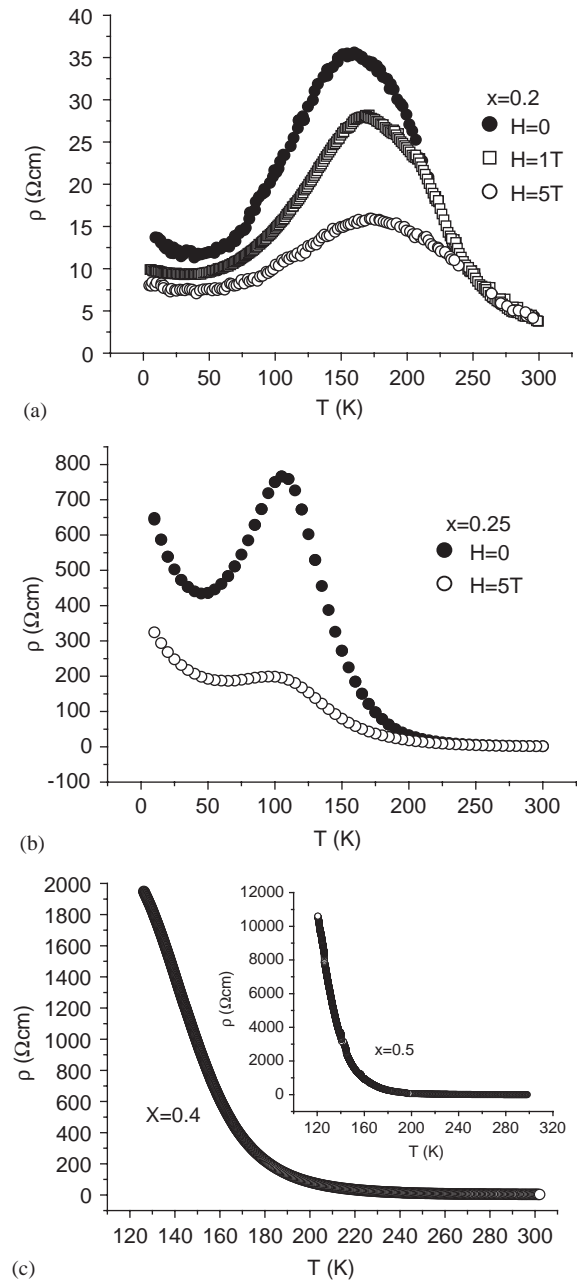


Fig. 3. Temperature-dependent resistivity  $\rho(T)$  of  $\text{La}_{1-x}\text{Bi}_x\text{MnO}_3$  samples measured under the magnetic field  $H = 0, 1$  and  $5\text{ T}$ . (a)  $x = 0.2$ , (b)  $x = 0.25$ , (c)  $H = 0$ ,  $x = 0.4$ , the inset shows the insulating behavior for  $x = 0.5$ .

$T_2 = 38\text{ K}$  (cooling measurement). For  $x = 0.25$ ,  $T_1 = 106\text{ K}$ ,  $T_2 = 45\text{ K}$  (cooling measurement). Similar MI transitions were observed in both

nonstoichiometric La manganites [19,24] and lightly doped manganites [25,26]. It should be noted that the metal-like state between  $T_1$  and  $T_2$  is unusual because the resistivity of this state is far above the Mott limit for metallic conduction. However, for simplicity, we call the transitions at  $T_1$  and  $T_2$  MI transitions. The MI transition temperature  $T_1$  is inconsistent with the ferromagnetic transition temperature  $T_c$ . Big differences between these two transition temperatures were also found in  $\text{LaMnO}_{3+\delta}$  [19] and  $\text{La}_{(2-x)/3}\text{Nd}_{x/3}\text{Ca}_{1/3}\text{MnO}_3$  [27]. Noticeable hysteretic behavior of resistivity is also identified in these two samples around  $T_1$  and  $T_2$  (not shown). The transition temperatures shift several Kelvins toward higher temperature side during the warming process. This hysteretic behavior was also found in other manganites [25].

When external magnetic fields are applied, the resistivity is reduced a lot. For  $x = 0.20$ , the transition temperature  $T_1$  shifts towards high temperature side, i.e.  $\Delta T_1 = 13.5\text{ K}$  at  $H = 1\text{ T}$  and  $\Delta T_1 = 17.4\text{ K}$  at  $H = 5\text{ T}$ . But the transition temperature  $T_2$  shifts towards low-temperature side, meaning that the insulating state below  $T_2$  in this sample can be suppressed under external fields although it cannot be completely suppressed even at  $H = 5\text{ T}$ . The magnetoresistance (MR) is negative and up to  $-59\%$  at  $H = 5\text{ T}$  (see Fig. 4(a)), where MR is defined as  $[\rho(H) - \rho(0)]/\rho(0)$ . Similar results were found in other manganites such as  $\text{La}_{0.94}\text{Mn}_{0.98}\text{O}_3$  [24] and  $\text{La}_{0.84}\text{Sr}_{0.16}\text{MnO}_3$  [26]. For  $x = 0.25$ , the shift of  $T_1$  is negligible, but  $T_2$  shifts towards high-temperature side, i.e.,  $\Delta T_2 = 15\text{ K}$  at  $H = 5\text{ T}$ . The negative MR is up to  $-74\%$  at  $H = 5\text{ T}$  (see Fig. 4(b)). Evidently, the insulating state below  $T_2$  in the  $x = 0.25$  sample is not suppressed but enhanced to appear at higher temperatures under external fields, opposite to that of the  $x = 0.20$  sample. This result was also found in lightly doped manganites  $\text{La}_{1-x}\text{Sr}_x\text{MnO}_3$  with  $x = 0.1-0.14$  [25].

#### 4. Discussion

As stated earlier, the role of the lone pair electrons of  $\text{Bi}^{3+}$  cannot be ruled out in these samples. Theoretical calculation [see Appendix A

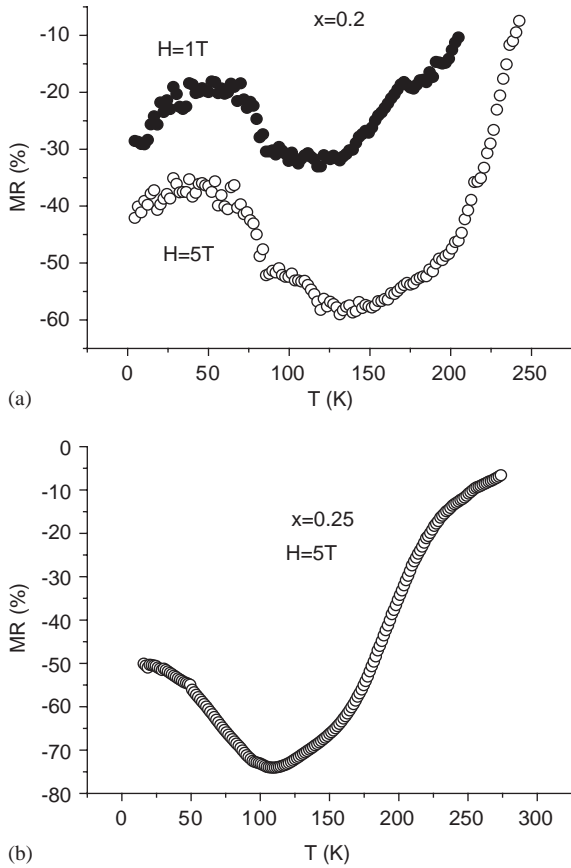


Fig. 4. Magnetoresistance  $MR = [\rho(H) - \rho(0)]/\rho(0)$  of (a)  $x = 0.2$ , (b)  $x = 0.25$ .

of Ref. [10] shows that off-center shifts of the ions with  $ns^2$  electronic configuration (hence, the structural distortion in a crystal) can take place to reach an energy reduction. So it has been proposed [12,13] that the lone pair preferentially orientates along a direction due to Coulomb repulsion with the ligand. The true situation might be rather of a covalent nature than purely ionic. If the electron density of the lone pair is high along some Bi–O bonds, then the lone pair electrons could be involved in the covalent interactions with Bi–O bonds, giving rise to a bigger effective ionic size of  $Bi^{3+}$ . In this case, the resistivity enhancement and magnetic frustration in LBMO are probably due to a partial hybridization of the Bi  $6s^2$  electrons with some O  $2p$  orbitals, which participate in the  $e_g-2p\sigma-e_g$  chemical bond. The partial hybridization could lead to carrier

localization by reducing the charge transfer of bonding  $e_g$  electrons from  $Mn^{3+}$  to  $Mn^{4+}$  ions, resulting in the increase of resistivity with increasing Bi-doping level. On the other hand, it could weaken the DE interaction, reducing  $T_c$ .

Another factor that may exert an influence on the magnetic and transport properties of LBMO is the existence of cationic vacancies. According to the published work [21], the potential fluctuations caused by cationic vacancies localize carriers, driving the system to evolve into an insulating state. On the other hand, it is likely that the ferromagnetic DE interaction is weakened due to the reduced mobility of carriers. Hence, the frustration of magnetization and the changes of resistivity behavior of LBMO may have some contribution from the existence of cationic vacancies. Until now, the role of cationic vacancies is not fully understood. There is disagreement among the published data. For example, according to Ref. [19], the saturation magnetization of  $LaMnO_{3+\delta}$  increases with  $\delta$  to a maximum value at around  $\delta = 0.12$ , but for  $\delta > 0.12$  it decreases with increasing  $\delta$ . When  $\delta \leq 0.13$ ,  $LaMnO_{3+\delta}$  displays insulating behavior, while for  $\delta = 0.14$  and  $0.18$  an MI transition is found at 130 K. The authors suggested that higher vacancy concentrations would result in samples showing MI transitions, as the carrier number was increased in order to overcome the competing effect of localization. However, according to Ref. [21], all samples of  $La_{1-x}Mn_{1-y}O_3$  with high vacancy concentrations ( $0.02 \leq x, y \leq 0.13$ ) show frustrated magnetization and insulating behavior, suggesting the localization effects outweigh the introduction of carriers. The vacancy concentration of the  $\delta = 0.18$  sample in Ref. [19] (equivalent to  $x = y = 0.057$ ) is even higher than that of the  $x = 0.022, y = 0.054$  sample in Ref. [21]. We think, one possible reason is that the role of Mn vacancies may be different from that of La-site vacancies because Mn vacancies more directly affect the ferromagnetic DE interactions. So further studies on the role of cationic vacancies are needed based on the accurate measurement of both La- and Mn-site vacancies other than the excess oxygen.

A remarkable feature in the resistivity curves for  $x = 0.2$  and  $0.25$  is the transition to the

ferromagnetic insulating (FI) state below  $T_2$ . The FI state can be frequently seen in manganites at low temperatures. There seem to be two kinds of FI states. One can be suppressed by applying external pressure or magnetic fields, i.e. the transition temperature  $T_{\text{FI}}$  shifts towards lower temperatures under pressure or magnetic fields and disappears at a strong enough pressure or magnetic field, just like that found in  $\text{La}_{0.94}\text{Mn}_{0.98}\text{O}_3$  [24] and  $\text{La}_{0.84}\text{Sr}_{0.16}\text{MnO}_3$  [26]. The other is enhanced by applying external pressure or magnetic fields, i.e.  $T_{\text{FI}}$  shifts towards higher temperatures under pressure or magnetic fields, just like that found in lightly doped manganites  $\text{La}_{1-x}\text{Sr}_x\text{MnO}_3$  ( $x = 0.1-0.14$ ) [25]. In LBMO, both kinds are observed. The first class appears in  $x = 0.2$  and the second in  $x = 0.25$ . The ferromagnetism in the insulating state cannot be understood only in the framework of DE interactions because the DE model predicts the coexistence of ferromagnetism and metallic nature. Moreover, the second class of FI state is unusual because it can be stabilized by applying external magnetic fields or pressure. The first class of FI state was thought to be due to the formation of a JT polaron lattice (clusters) at lower temperatures ( $T \leq T_{\text{FI}}$ ) [26]. The JT polarons are thermally activated and barely mobile when  $T_{\text{FI}} \leq T \leq T_c$ , but are weakly localized when  $T \leq T_{\text{FI}}$ . The weakly localized  $e_g$  carriers can mediate the DE interaction between the neighboring  $t_{2g}$  spins and cause the ferromagnetic state. The origin of the second class of FI state was explained as the ferromagnetic superexchange (SE) interaction induced by an antiferromagnetic-type orbital ordering, which accompanies carrier localization [17]. The SE interaction is strongly dependent on the orbital overlapping integrals, which in turn are expected to be enhanced under pressure or magnetic fields. Therefore,  $T_{\text{FI}}$  shifts to higher temperatures. The orbital ordering in this FI state occurs only when the cooperative JT distortion is absent or significantly reduced. As the cooperative JT distortion is thought to be greatly reduced in our rhombohedral samples, it seems that this kind of orbital ordering could occur and be responsible for the FI state at low temperature in our  $x = 0.25$  sample. However, for  $x = 0.2$ , which is also

rhombohedral, we observe the first class of FI state not the second one. This suggests that instead of antiferromagnetic-type orbital ordering, JT polaron ordering develops in  $x = 0.2$ . It seems that the change from orbital ordering to polaron ordering is due to the change of the mobility or density of carriers. Similar results were found in  $\text{La}_{1-x}\text{Sr}_x\text{MnO}_3$  system [25,26]. When  $x > 0.14$  the FI state changes from the second class to the first. So if the above interpretation is essentially correct, electron–lattice coupling plays significant roles in these structural transitions at  $T_{\text{FI}}$ . This topic remains for further investigations.

Our work shows that the addition of Bi is detrimental to the DE interaction. This may seem inconsistent with the fact that  $\text{BiMnO}_3$  is ferromagnetic. However, the ferromagnetic ordering in  $\text{BiMnO}_3$  is most probably not caused by the DE interaction. Published work supports this viewpoint. Any hole doping (i.e. introduction of  $\text{Mn}^{4+}$ ) by partly replacing Bi with Ca or Sr [13,14] does not enhance ferromagnetism. Instead, it usually induces charge ordering, destroying ferromagnetic ordering rapidly. Recently, Atou et al. [12] have proposed a new kind of orbital ordering for the ferromagnetism of  $\text{BiMnO}_3$ , in which two-thirds of the Mn–O–Mn orbital configurations are favorable for ferromagnetism via superexchange interaction. Superexchange interactions were also suggested to be responsible for the ferromagnetism in  $\text{Mn}^{3+}$ -free manganites  $\text{Tl}_2\text{Mn}_2\text{O}_7$  [28] and  $\text{CaCu}_3\text{Mn}_4\text{O}_{12}$  [29].

In conclusion, we observed a series of changes in structure, magnetic and transport properties of LBMO caused by Bi doping. The Bi  $6s^2$  lone pair electrons and the existence of cationic vacancies are suggested to be two important factors, which localize carriers, weaken the DE interactions and therefore drive the system to evolve towards an insulating magnetic glass. Two kinds of ferromagnetic insulating (FI) states were found in low temperatures. They are two structural phases with long-range orbital ordering and polaron ordering, respectively.

## Acknowledgments

We would like to thank Prof. Z.G. Khim and Prof. K. Char for permission to use the SQUID and

resistivity measurement systems. We also thank Dr. Y.-J. Doh, Mr. S.-Y. Lee and Mr. S.H. Jeon for their help in resistivity and magnetization measurements.

## References

- [1] R. von Helmolt, J. Wecker, B. Holzapfel, L. Schultz, K. Samwer, *Phys. Rev. Lett.* 71 (1993) 2331.
- [2] K. Chahara, T. Ohno, M. Kasai, Y. Kosono, *Appl. Phys. Lett.* 63 (1993) 1990.
- [3] S. Jin, T.H. Teifel, M. McCormack, R.A. Fastnacht, R. Ramesh, L.H. Chen, *Science* 264 (1994) 413.
- [4] Y. Yamada, O. Hino, S. Nohdo, R. Kanao, T. Inami, S. Katano, *Phys. Rev. Lett.* 77 (1996) 904.
- [5] J.B. Goodenough, *Phys. Rev.* 100 (1955) 564; E.O. Wollan, W.C. Koehler, *Phys. Rev.* 100 (1955) 545.
- [6] P.Ge. de Gennes, *Phys. Rev.* 118 (1960) 141; P.W. Anderson, H. Hasegawa, *Phys. Rev.* 100 (1955) 675; C. Zener, *Phys. Rev.* 82 (1951) 403.
- [7] H.Y. Hwang, S.-W. Cheong, P.G. Radaelli, M. Marezio, B. Batlogg, *Phys. Rev. Lett.* 75 (1995) 914.
- [8] L.M. Rodriguez-Martinez, J.P. Atteld, *Phys. Rev. B* 54 (1996) 15622; L.M. Rodriguez-Martinez, J.P. Atteld, *Phys. Rev. B* 58 (1998) 2426; L.M. Rodriguez-Martinez, J.P. Atteld, *Phys. Rev. B* 63 (2001) 024424; L.M. Rodriguez-Martinez, J.P. Atteld, *Chem. Mater.* 11 (1999) 1504.
- [9] A. Maignan, C. Martin, G. Van Tendeloo, M. Hervieu, B. Raveau, *Phys. Rev. B* 60 (1999) 15214.
- [10] F. Sugawara, S. Iida, Y. Syono, S. Akimoto, *J. Phys. Soc. Jpn.* 25 (1968) 1553; F. Sugawara, S. Iida, Y. Syono, S. Akimoto, *J. Phys. Soc. Jpn.* 20 (1965) 1529.
- [11] H. Chiba, T. Atou, Y. Syono, *J. Solid State Chem.* 132 (1997) 139.
- [12] T. Atou, H. Chiba, K. Ohoyama, Y. Yamaguchi, Y. Syono, *J. Solid State Chem.* 145 (1999) 639.
- [13] J.L. Garcia-Munoz, C. Frontera, M.A.G. Aranda, A. Llobet, C. Ritter, *Phys. Rev. B* 63 (2001) 064415.
- [14] H. Woo, T.A. Tyson, M. Croft, S.-W. Cheong, J.C. Woicik, *Phys. Rev. B* 63 (2001) 134412.
- [15] I.O. Troyanchuk, N.V. Kasper, O.S. Mantyskaya, S.N. Pastushonok, *JETP* 78 (1994) 212.
- [16] R.D. Shannon, *Acta Crystallogr., Sec. A* 32 (1976) 751; R.D. Shannon, C.T. Prewitt, *Acta Crystallogr., Sec. B* 25 (1969) 925.
- [17] H. Nojiri, K. Kaneko, M. Motokawa, K. Hirota, Y. Endoh, K. Takahashi, *Phys. Rev. B* 60 (1999) 4142; Y. Endoh, K. Hirota, S. Ishihara, S. Okamoto, Y. Murakami, A. Nishizawa, T. Fukuda, H. Kimura, H. Nojiri, K. Kaneko, S. Maekawa, *Phys. Rev. Lett.* 82 (1999) 4328.
- [18] A. Wold, R. Arnott, *J. Phys. Chem. Solids* 9 (1959) 176.
- [19] J. Topfer, J.B. Goodenough, *J. Solid State Chem.* 130 (1997) 117.
- [20] J.A.M. Van Roosmalen, E.H.P. Cordfunke, R.B. Helmholtz, H.W. Zandbergen, *J. Solid State Chem.* 110 (1994) 100.
- [21] P.S.I.P.N. de Silva, F.M. Richards, L.F. Cohen, J.A. Alonso, M.J. Martinez-lope, M.T. Casais, K.A. Thomas, J.L. MacManus-Driscoll, *J. Appl. Phys.* 83 (1998) 394 and the references therein.
- [22] J.A. Mydosh, *Spin Glasses*, Taylor & Francis, London, 1993.
- [23] R.S. Freitas, L. Ghivelder, F. Damay, F. Dias, L.F. Cohen, *Phys. Rev. B* 64 (2001) 144404.
- [24] V. Markovich, E. Rozenberg, G. Gorodetsky, M. Greenblatt, W.H. McCarroll, *Phys. Rev. B* 63 (2001) 054423.
- [25] R. Senis, V. Laukhin, B. Martinez, J. Fontcuberta, X. Obradors, A.A. Arsenov, Y.M. Mukovskii, *Phys. Rev. B* 57 (1998) 14680; B. Martinez, R. Senis, Ll. Balcells, V. Laukhin, J. Fontcuberta, L. Pinsard, A. Revcolevschi, *Phys. Rev. B* 61 (2000) 8643.
- [26] Y. Moritomo, A. Asamitsu, Y. Tokura, *Phys. Rev. B* 56 (1997) 12190.
- [27] G.H. Rao, J.R. Sun, J.K. Liang, W.Y. Zhou, *Phys. Rev. B* 55 (1997) 3742.
- [28] M.A. Subramanian, B.H. Toby, A.P. Ramirez, W.J. Marshall, A.W. Sleight, G.H. Kwei, *Science* 273 (1996) 81.
- [29] Z. Zeng, M. Greenblatt, M.A. Subramanian, M. Croft, *Phys. Rev. Lett.* 82 (1999) 3164.